IEEE Access
Multidisciplinary | Rapid Review | Open Access Journal

Received 25 May 2022, accepted 23 June 2022, date of publication 4 July 2022, date of current version 11 July 2022.

Digital Object Identifier 10.1109/ACCESS.2022.3188099

RESEARCH ARTICLE

A Laser Intensity Based Autonomous Docking Approach for Mobile Robot Recharging in Unstructured Environments

YUGANG LIU, (Member, IEEE)
Department of Electrical and Computer Engineering, Royal Military College of Canada, Kingston, ON K7K 7B4, Canada
e-mail: yugang.liu@rmc-cmr.ca

This work was supported by the Canadian Defence Academy Research Program.

ABSTRACT Autonomous recharging is a fundamental requirement for autonomous mobile robots in order to allow them to work continuously without human intervention, and autonomous docking to a charging station is a challenging yet promising research area. In particular, the docking task becomes even more complicated in unstructured human environments when the charging station's location is not fixed and when there are dynamic obstacles moving around. This paper presents a laser intensity based autonomous docking approach, which allows a mobile robot to recharge its battery autonomously in unstructured environments. Laser reflection intensity for a self-adhesive reflective tape is quantitatively investigated, and the sufficient/necessary conditions for successful reflector detection are discussed. Using the proposed reflector detection technique, the charging station can be easily distinguished from similar objects in an unstructured environment. Comparing to the traditional docking methods, the developed approach is easier to implement and can significantly improve the reliability of autonomous docking and recharging. Extensive experiments were conducted to verify the effectiveness of the developed autonomous docking approach.

INDEX TERMS Autonomous docking, laser intensity, mobile robots.

I. INTRODUCTION

Autonomous mobile robots have substantial application potentials in such areas as warehouse automation [1], personal care [2], surveillance and patrolling [3], planetary exploration [4] as well as search and rescue operations [5]–[7]. In order to enable continuous working without human intervention, power supply has been an important concern. A typical rechargeable battery can provide power supply for a mobile robot for a few hours of peak usage, and has to be recharged before becoming exhausted [8]. As a result, autonomous recharging has become a fundamental requirement for autonomous mobile robots. In order to start the recharging process, a mobile robot needs to identify and dock to the charging station autonomously, which are complicated tasks in unstructured environments.

Autonomous docking is a challenging yet promising research topic, which attracted extensive research attention. According to the sensors implemented, the autonomous docking techniques reported in the literature can be categorized into infrared range (IR) sensor based methods, vision-based algorithms, and laser-based approaches. In order to improve the reliability of autonomous docking, many researchers selected to integrate IR sensors or cameras with laser range finders.

IR-based autonomous docking methods rely on communication between the IR transmitters which were normally mounted on the charging station and the IR receivers that were usually attached to the mobile platform, in order to guide the mobile robot to the docking location [9]. The IR sensor based methods are affordable and easy to implement. However, the IR receivers need to be installed at a specific location on the mobile platform in order to guarantee that IR signals from the IR emitters of the charging station can be received properly, which put a limitation to the mechanical design of the mobile platform.

Vision-based autonomous docking algorithms rely on visual pattern recognition, and artificial landmarks, tags or

The associate editor coordinating the review of this manuscript and approving it for publication was Wai-Keung Fung.

quick response (QR) codes are normally utilized in order to simplify the detection of charging stations [3], [10], [11]. The camera does not have to be installed at the same height as the charging station, relaxing the requirement on mobile robot design. However, vision-based approaches are prone to errors induced by camera calibration or varying lighting conditions. Furthermore, a small error at the charger's relative location with respect to the aforementioned landmarks can fail the autonomous docking operations.

Laser-based autonomous docking approaches detect the docking stations through their contours, which are normally designed to be with special shapes in order to make them stand out from the background [12]. Furthermore, the traditional laser based techniques usually have strong requirements on the docking station's surrounding environment [13], limiting their applications in unstructured environments.

In order to address the limitations of conventional autonomous docking techniques, laser intensity information is introduced, for the first time, to detect the docking station in this paper. The novel laser-intensity based autonomous docking approach has the below advantages:

- ☐ Comparing to the IR-based methods, laser-based autonomous docking approaches can make use of the onboard laser range finders that were already equipped for localization and mapping purposes, and no extra onboard hardware needs to be introduced.
- ☐ Unlike vision-based algorithms, laser-based autonomous docking approaches are not affected by the lighting conditions, and can accommodate the variance in the charger's location.
- ☐ Using laser-intensity information, the proposed autonomous docking approach can easily detect the charging station from an unstructured environment, without any requirements on the charger's shape or the contour of objects in its adjacent area.
- ☐ Furthermore, attaching two pieces of reflective tape to a charging station is much easier and more affordable than fabricating docking station with special shapes. Thus, the proposed laser-intensity based autonomous docking approach is easier to deploy than the traditional laser-based docking techniques.

The remaining part of this paper consists of five sections, and the following section provides a detailed overview of the related work on autonomous docking and recharging, as well as laser intensity based mobile robot applications. In section III, the sufficient and necessary conditions for successful reflector detection are discussed, and a laser intensity based reflector detection technique is proposed. Section IV presents the development of a laser-intensity based autonomous docking approach. Experimental results are presented in Section V, and concluding marks are given in Section VI.

II. RELATED WORK

A. AUTONOMOUS DOCKING AND RECHARGING OF MOBILE ROBOT SYSTEMS

The research on mobile robot recharging can be traced back to 1950s, when the first autonomous recharging mobile robots were developed, which utilized a light beacon to guide the mobile robots to a battery re-charger that was mounted inside a hutch [14]. Most of the modern autonomous recharging techniques were developed based on similar ideas, i.e., using sensors to detect a charging station and assist the docking process [8]. This subsection provides an overview of the related research work on autonomous docking and recharging based on the different sensors implemented.

In related researches on IR-based methods, three infrared transmitters and three infrared receivers were utilized for autonomous docking and recharging of a mobile robot [9]. In the proposed method, the global navigation space was separated into docking and working spaces using the three IR transmitters. Furthermore, the mounting locations and orientations of the three IR receivers were investigated in order to minimize the docking time. The developed algorithm was verified by extensive experiments in a laboratory. In [15], two IR LED emitters were fixed on the docking station and one IR receiver was installed at the back of the mobile robot in order to enable the autonomous homing process. In order to compensate for the lateral and directional docking errors, two novel docking mechanisms were proposed using friction or magnetic forces between the docking parts of the mobile robot and those of the docking station. The proposed algorithm was proven to be effective through experiments.

As for vision-based algorithms, an autonomous docking and recharging system was proposed for mobile robots in warehouse environments in [1]. In order to assist the mobile robot to find the charging station, a fiducial marker system called AprilTag was implemented, which was attached above the charging station. The algorithm worked by extracting the marker from the image taken by the onboard camera, calculating the coordinates of the four vertices of the marker, and determining the edge of the marker through an image recognition technology. The experimental results indicated that the developed algorithm worked well in warehouse environments, but the change in lighting conditions and the shielding of tags could interrupt the docking process. In [3], a vision-based autonomous docking and recharging system was developed for a security robot. In order to assist the security mobile robot to detect the charging station, a navy blue circular landmark with known diameter was installed on top of the docking station at the same height as the onboard camera. The vision system was implemented to detect the artificial landmark and locate the site of the charging station. To accommodate the horizontal and rotational docking errors, a virtual spring based control approach was proposed, which assumed that the robot and the docking station be connected by a virtual spring and the motion control was determined by the compliant forces in the direction of the

translation deformation and bending. The effectiveness of the proposed docking control approach was validated via experiments.

With respect to laser-based techniques, MiR (mobile industrial robots) reserved a V-shaped recess on its $24V$ charger in order to help the onboard laser range finder to detect the charging station [12]. Similarly, Fetch robotics required its charging dock to be separated from any sort of laser-height obstacles in order to allow the laser range finder to successfully detect the profile of the charging station [13]. The cut of V-shaped recess on the MiR charger increases fabrication cost of the charging station, and the requirement of Fetch robotics' recharging process will limit the robot's practical applications in unstructured environments.

In order to address the limitations of IR-based, vision-based or laser-based techniques, many researches selected to use multiple sensors for autonomous docking and recharging. For example, in [8], a pan-tilt-zoom (PTZ) camera was implemented to find the docking station, and a laser range finder was utilized to determine the robot's angle to the wall in order to orient the robot with the docking station. Furthermore, IR-LED was employed to determine whether the autonomous docking operation was successful. In order to assist the mobile robot to detect the charging station, an orange colored pieced paper was mounted on top of the docking station as the artificial landmark. A laser beacon was attached below the artificial landmark but above the charging station in order to assist the mobile robot with its orientation. The proposed technique was verified through experiments using a Pioneer mobile platform. In [16], QR codes were implemented as visual landmarks in order to guide the mobile robot to the charging dock, and IR sensors were utilized for distance measurement in order to assist the docking process. Based on the IR measurements, the docking area were defined into three regions, and different approaching strategies were defined for each region. The effectiveness of the developed approach was demonstrated through experiments. In [17], ultrasonic sensors and IR sensors were implemented for autonomous docking and recharging of a wheeled mobile robot. In the proposed approach, ultrasonic sensors were utilized to detect the charging station and estimate distance from it and IR sensors were employed to tune the orientation of the mobile robot at the exact position for docking purpose. The effectiveness of the proposed approach was validated through experiments.

With the development of machine learning techniques, the focus of research on autonomous docking has transferred from static and structured environments to dynamic and unstructured environments. In [18], convolutional neural networks (CNN) were implemented for pattern detection of charging station in RGB (red, green, blue) images. The detected patterns together with 2D laser scans and images were fed to a reinforcement learning (RL) technique to produce such actions as translations, rotations or tilting cameras. Experimental results confirmed the effectiveness of the proposed approach with a success rates of about 100% in obstacle-free environments and 93% in cluttered paths. In [19], autonomous docking of an automated guided vehicle (AGV) was investigated in unstructured human environments, which utilized Lidar and AprilTag for autonomous docking to a workstation and adopted deep learning network for human detection and recognition. Practical experiments demonstrated that the proposed approach could control an intelligent AGV to co-exist with human workers and conduct autonomous docking tasks in unstructured environments.

B. LASER INTENSITY FOR MOBILE ROBOT APPLICATIONS

Laser range finders have been widely implemented in mobile robot systems, and the range information has been extensively utilized for obstacle detection as well as simultaneous localization and mapping (SLAM). Besides range information, laser range finders can also provide reflection intensity for each laser beam, which is the optical power received after reflection from the surface [20]. Comparing to laser range based studies, the researches on laser intensities are relatively rare, and the few papers published had been focusing on SLAM [20], [21] and people detection [22]. This subsection works as a short survey regarding laser intensity based mobile robot applications.

In [20], a data-driven modeling approach was proposed to investigate the influence of extrinsic parameters on laser intensities, which was coupled with extended Hector SLAM in order to generate a reflectivity map of the environment. Experimental results confirmed that the reflectivity based SLAM technique is effective when metric information is not sufficient for pose estimation and consistent map generation.

In [21], materials with different reflection intensities were utilized as artificial landmarks in order to improve the localization performance of mobile robots in featureless environments. The reflection intensity from the landmarks was fused with the geometric information of the environment, in order to improve the traditional scan-matching algorithms. The proposed scan-matching algorithm was proven to be more accurate and more robust than the traditional scan-matching techniques in such featureless environments as corridors.

In [22], laser reflection intensity was implemented to improve the people detection performance for a mobile robot using multi-layered laser range finders. In the proposed approach, laser reflection intensity was implemented to train a strong classifier to detect body parts, to combine candidate segments, and to separate merged segments. The effectiveness of the proposed approach was verified by experiments.

In [23], a novel SLAM framework was proposed using both geometry and intensity features. In the proposed approach, laser intensities were implemented for both front-end odometry estimation and back-end optimization. Experiments were conducted for localization and mapping in both indoor warehouse environments and outdoor autonomous driving scenarios, and the experimental results confirmed that the introduction of intensity information significantly improved the localization accuracy.

C. LITERATURE SUMMARY

As can be seen from the previous sub-sections, extensive efforts have been reported in the literature towards developing reliable autonomous docking and recharging techniques for mobile robot systems. The novel contributions of this paper can be summarized as below:

- ☐ In the author's knowledge, laser intensity information has never been directly implemented for autonomous docking. This paper, for the first time, presents the development a laser intensity based autonomous docking approach, allowing for autonomous recharging of mobile robots in unstructured environments.
- ☐ As the author know, sufficient and necessary conditions for successful reflector detection have never been reported in the literature. In this paper, these conditions were derived, which will significantly benefit reflector installation in practical applications.
- ☐ Retro-reflective material and black rubbers are known to have different reflection properties. However, their influence on laser intensity has not been quantitatively reported. In this paper, experiments were conducted to quantitatively investigate the laser reflection intensity of a reflective tape.
- ☐ Most of the autonomous docking techniques reported in the literature were tested in structured environments. This paper conducted physical experiments in unstructured environments, testing the influence of charger location uncertainty, moving obstacles and objects with similar contour in the charger's adjacent area.

III. LASER INTENSITY BASED REFLECTOR DETECTION

The mobile platform utilized in this paper is the bottom part of a service robot, which was developed for greeting, hosting and guiding customers in libraries, banks, and airports, as shown in Fig. 1(a) and 1(b). The mobile platform is equipped with a SICK TiM571 laser range finder and four pairs of ultrasound sensors, as shown in Figs. 1(a) and 1(b). In order to improve the reliability of autonomous docking, two pieces of self-adhesive reflective tapes were attached to the charging station, as shown in Fig. 1(c). Each reflective tape consists of three sections. The middle section is made of diamond retro-reflective material and the two outer ones are made of black rubbers, as shown in Fig. 1(d).

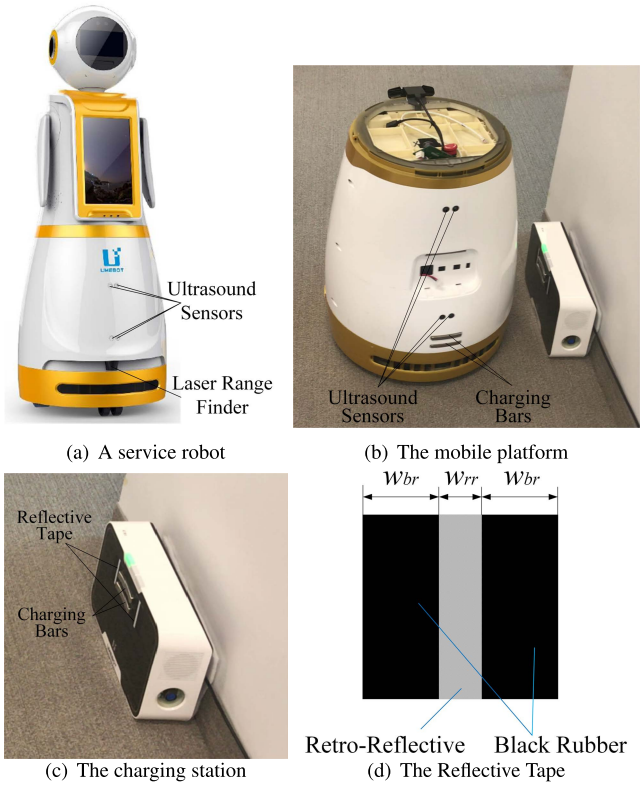

(a) A service robot (b) The mobile platform (c) The charging station (d) The Reflective Tape

FIGURE 1. Mobile robot and the charging station.

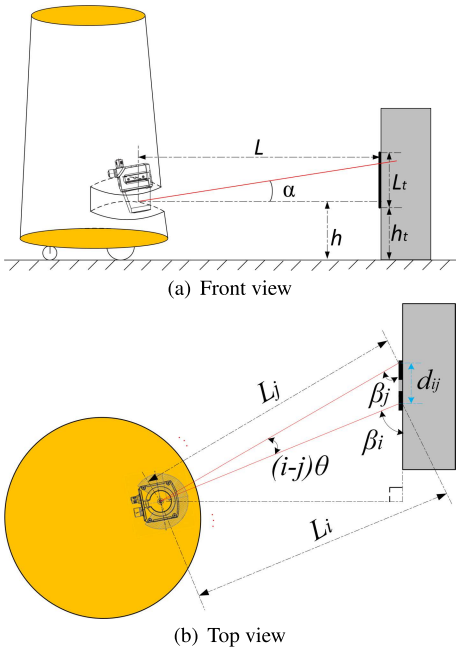

(a) Front view (b) Top view

FIGURE 2. Sufficient and necessary conditions for reflective tape detection.

A. SUFFICIENT AND NECESSARY CONDITIONS FOR REFLECTOR DETECTION

In order to reliably detect a reflective tape in an unstructured environment, one or more laser beams from the laser range finder need to be reflected from the retro-reflective area and the black-rubber regions, respectively. In this subsection, sufficient and necessary conditions for successful detection of the reflective tapes are discussed.

Each laser range finder has a working range, which is normally identified in its specification. For example, the working range for SICK TiM571 is from 0.05m to 25m [24]. In order to successfully detect a reflective tape, a mobile robot needs to be in a location where the distance between its onboard laser range finder (LRF) and the reflective tape is within the working range of the LRF. Similarly, the reflective tapes needs to be placed at the same height as where the

laser beams can reach. In practical applications, the laser range finder may be slightly tilted up from the horizontal plane, in order to avoid scanning the floor during the mapping process. In such a scenario, the reflective tapes needs to be long enough to cover the different heights that the laser beam can reach when the mobile robot situates at different detecting locations, as shown in Fig. 2(a). These are obvious but necessary conditions for successful detection of the reflective tape, which can be summarized as follows:

$$\begin{aligned} L_{min}\cos\alpha \le L \le L_{max}\cos\alpha \quad (a)\\ h - L_t + L\cdot\tan\alpha \le h_t \le h \quad (b) \end{aligned} \tag{1}$$

where L_{min} and L_{max} denote the minimum and maximum working range of the laser range finder; L is the distance between the laser range finder and the reflective tape; α is the tilting angle of the laser range finder with respect to the horizontal plane; h represents the height of the laser emitter with respect to the ground; and h_t, L_t are the installation height and the length of the reflective tape, respectively.

Equation (1) defines the necessary conditions, i.e., the fundamental requirements for reflective tape detection. In order to derive the sufficient conditions, the distance between two adjacent laser beams need to be analyzed. Assume laser beam i and j are both reflected from the reflective tape, from Fig. 2(b), we can obtain

$$\begin{aligned} L_i\sin\beta_i = L_j\sin\beta_j \quad (a)\\ \beta_i - \beta_j = (i-j)\,\theta \quad (b) \end{aligned} \tag{2}$$

where β_i and β_j represent the inception angles of the laser beams, i.e., the angles between the laser beams and the reflective tape; L_i and L_j, denote the measured ranges for laser beam i and j, respectively; θ is the angular resolution of the laser range finder, which is a constant and can be found from its specification.

Submitting (2b) into (2a), we can obtain

$$\begin{aligned} \beta_i = \arctan\left\{\frac{L_j\sin\left[(i-j)\,\theta\right]}{L_j\cos\left[(i-j)\,\theta\right] - L_i}\right\} \quad (a)\\ \beta_j = \arctan\left\{\frac{L_j\sin\left[(i-j)\,\theta\right]}{L_j - L_i\cos\left[(i-j)\,\theta\right]}\right\} \quad (b) \end{aligned} \tag{3}$$

Remark 1: In (3), the angular resolution θ is a constant, and the laser beam indexes i, j as well as the ranges L_i, L_j can be obtained from the scan data. Therefore, (3) can be utilized for online inception angle estimation for each laser beam reflected from the reflective tape. These inception angles can be further utilized to determine the position of the reflective tape with respect to the coordinate system that is fixed on the mobile platform.

From Fig. 2, the distance between the reflection points of laser beams i and j can be calculated by:

$$\begin{aligned} d_{ij} = L_j\cos\beta_j - L_i\cos\beta_i \quad (a)\\ d_{ij} = \sqrt{L_i^2 + L_j^2 - 2L_iL_j\cos\left[(i-j)\,\theta\right]} \quad (b) \end{aligned} \tag{4}$$

For two adjacent laser beams reflected from the reflective tape, $i = j + 1$. In order to have more than one laser beams reflected from the middle retro-reflective region and each black rubber section of the reflective tape, there should be at least one laser beam i and one laser beam j that satisfy the following conditions:

$$\begin{aligned} d_{i-1,i} = \sqrt{L_i^2 + L_{i-1}^2 - 2L_iL_{i-1}\cos\theta} < w_{rr} \quad (a)\\ d_{j-1,j} = \sqrt{L_j^2 + L_{j-1}^2 - 2L_jL_{j-1}\cos\theta} < w_{br} \quad (b) \end{aligned} \tag{5}$$

where w_{rr} and w_{br} represent the widths of the retro-reflective and black rubber sections, respectively, as shown in Fig. 1(d).

Submitting $j = i - 1$ into (2) and (5), we can obtain

$$\begin{aligned} \frac{L_{i-1}}{L_i} = \frac{\sin\left(\beta_{i-1} + \theta\right)}{\sin\beta_{i-1}} \quad (a)\\ d_{i-1,i} = L_{i-1}\cdot\cos\beta_{i-1} - L_i\cdot\cos\left(\beta_{i-1} + \theta\right) \quad (b) \end{aligned} \tag{6}$$

Remark 2: When the inception angle is very small, i.e., $\beta_{i-1} \to 0, \beta_{j-1} \to 0$, from (6) we can obtain $\frac{L_{i-1}}{L_i} \to \infty$ and $w_{rr} \ll d_{i-1,i} \to \infty, w_{br} \ll d_{j-1,j} \to \infty$, which indicate that the reflective tape cannot be detected. The aforementioned analysis explained the influence of laser beam inception angles on reflective tape detection, which was incorporated in the conditions listed in (5).

In practical applications, the laser angular resolution is normally very small. For example, the angular resolution for SICK TiM571 is $\theta = 0.33° \approx 0.00576\ rad$. As a result, In most of the scenarios, it is reasonable to assume that the inception angle β_{i-1} is much bigger than the laser angular resolution, i.e., $\beta_{i-1} \gg \theta$. From (6a), we can obtain $L_{i-1} \approx L_i$. Submitting this equation into (5) yields

$$\begin{aligned} d_{i-1,i} \approx 2L_i\sin\frac{\theta}{2} < w_{rr} \quad (a)\\ d_{j-1,j} \approx 2L_j\sin\frac{\theta}{2} < w_{br} \quad (b) \end{aligned} \tag{7}$$

Remark 3: Equation (7) provides us with a method to roughly estimate the required distance for successful reflective tape detection, and the number of laser beams reflected from different sections of the reflective tape, i.e.,

$$\begin{aligned} L \le \frac{\min\left(w_{rr}, w_{br}\right)}{2\sin\frac{\theta}{2}} \quad (a)\\ n_{rr} = \left\lfloor\frac{w_{rr}}{2\sin\frac{\theta}{2}}\right\rfloor \quad (b)\\ n_{br} = \left\lfloor\frac{w_{rr}}{2\sin\frac{\theta}{2}}\right\rfloor \quad (c) \end{aligned} \tag{8}$$

where n_{rr} and n_{br} represent the number of laser beams reflected from the retro-reflective and black rubber sections of the reflective tape, respectively

B. A LASER INTENSITY BASED REFLECTOR DETECTION ALGORITHM

Based on the aforementioned analysis, a laser intensity based reflector detection algorithm is proposed, as shown in Fig. 3. Herein, n_{det} represents the number of detected reflectors;

n_{ref} is the number of installed reflectors; n_{beam} denotes the number of laser beams, which can be calculated using the aperture angle and angular resolution of the laser range finder. Similar as the angular resolution, the aperture angle is also listed in the specification of laser range finders. For example, the aperture angle for SICK TiM571 is 270° [24]. $I[i]$ is the measured SICK intensity value for laser beam i; I_{max} and I_{min} denote the maximum and minimum SICK intensity values, which are measured by laser beam i_{max} and i_{min}, respectively; I_{peak} and I_{valley} are the thresholds for the peak and valley detection in the laser intensity curve.

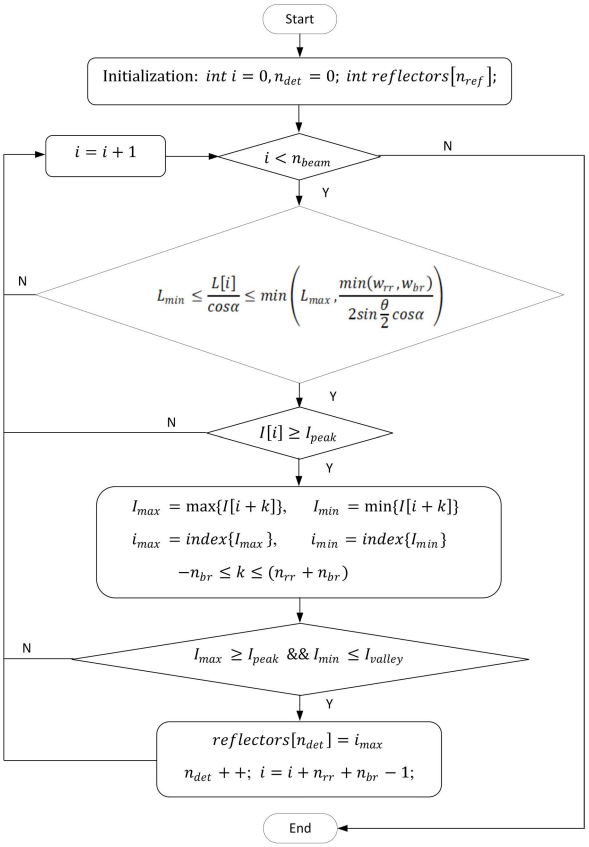

FIGURE 3. Laser intensity based reflector detection algorithm.

IV. LASER INTENSITY BASED AUTONOMOUS DOCKING

The mobile robot generates maps using GMapping [25] and conducts autonomous navigation using ROS (robot operating system) navigation stack [26]. The charging station is put against a wall, as shown in Fig. 1(c). It is not fixed and can be moved along the wall within a specific range, which is limited by the length of the power cord. A point that is located at $0.8m$ in front of the charging station is defined as the charging waypoint in the generated map, and the mobile platform navigates towards the charging waypoint autonomously when the battery level is low or when a recharging command is received from the operator. Autonomous navigation to a waypoint inside a known map is not our focus, and will not be detailed in this paper. This section presents a laser intensity based autonomous docking approach, which determines the motion of the mobile platform, starting from the aforementioned charging waypoint.

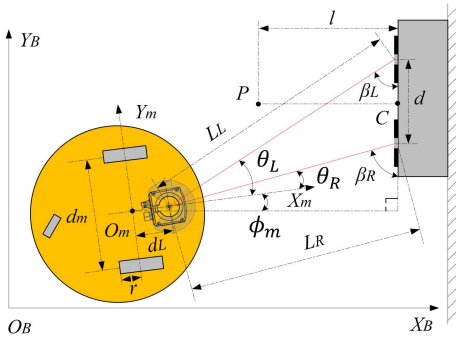

FIGURE 4. Coordinate system definition.

The mobile platform implemented in this paper is a differential drive wheeled mobile robot, which was designed to move on a horizontal plane, as shown in Fig. 4. The coordinate systems are defined as follows: O_B-$X_BY_BZ_B$ forms the inertial base frame, and O_m-$X_mY_mZ_m$ is a frame fixed on the mobile platform. The origin O_B is selected to be at the aforementioned charging waypoint, and O_BX_B is vertical with the wall. $O_m(x_m, y_m)$ is defined at the midpoint of the line segment connecting the two driving wheel centers, and O_mY_m is along the coaxial direction of the two driving wheels. ϕ_m is the angle between O_mX_m and O_BX_B, which determines the heading direction of the mobile platform. In Fig. 4, L_L, L_R, β_L and β_R represent the ranges and inception angles of the strongest laser beams reflected from the two left-side and right-side reflective tapes, respectively. d is the distance between the central lines of the two reflective tapes. d_m denotes the tread width of the mobile platform, i.e., the distance between the two driving wheels. r is the radius of the driving wheels. d_L is the offset of the laser range finder with respect to O_m along the O_mX_m direction.

Define $C(x_c, y_c, z_c)$ as the center of the charging bars, from Fig. 2(a) and Fig. 4, we can obtain:

$$x_c = x_m + d_L \cos\phi_m + L_L \cos\alpha \sin\beta_L \quad (a)$$
$$y_c = y_m + d_L \sin\phi_m + L_L \cos\alpha \cos\beta_L - \frac{d}{2} \quad (b)$$
$$\beta_L + \theta_L + \phi_m = \frac{\pi}{2} \quad (c) \quad (9)$$

Remark 4: In (9), $x_c = 0.8m$; α, d_L and d are constants; y_c may vary, but will keep constant during each experiment; θ_L and β_L can be derived from the scan data, as discussed in Remark 1. Thus, x_m, y_m and ϕ_m can be calculated online using the scan information in each experiment. This laser intensity based localization approach can be integrated with wheel odometry using extended Kalman filters, which will not be detailed here.

The charging bars are fixed in the back of the mobile platform implemented in this paper, while the laser range finder is installed in the front side, as shown in Figs. 1(a) and (b).

In order to achieve autonomous docking, an intermediate point $P(x_m^p, y_m^p)$ is introduced, which is selected at $x_m^p = x_c - l$ and $y_m^p = y_c$, as shown in Fig. 4. Herein l is a constant, which needs to be longer than the turning radius of the mobile platform in order to avoid colliding with the charging station. The idea is to control the mobile robot to the intermediate point P with the orientation of $\phi_m^p = \pi$, and then back the robot into the charging location.

The control inputs of the mobile platform are the linear and angular velocities, namely v and ω. The system equation can be given by

$$\begin{bmatrix} \dot{x}_m \\ \dot{y}_m \\ \dot{\phi}_m \end{bmatrix} = \begin{bmatrix} \cos\phi_m & 0 \\ \sin\phi_m & 0 \\ 0 & 1 \end{bmatrix} \cdot \begin{bmatrix} v \\ \omega \end{bmatrix} \tag{10}$$

In order to control the mobile platform to the intermediate location P, the mobile platform is controlled with the following steps: (1) to turn towards the intermediate point P, (2) to move towards the intermediate point along a straight line, and (3) to turn towards to desired orientation ϕ_m^p. During these motions, proportional controllers were implemented:

$$\begin{aligned} \omega(t) &= k_1\left[\phi_m^p - \phi_m(t)\right] \quad (a) \\ v(t) &= k_2\sqrt{\left[x_m^p - x_m(t)\right]^2 + \left[y_m^p - y_m(t)\right]^2} \quad (b) \end{aligned} \tag{11}$$

where $k_1 = 0.8$ and $k_2 = 0.5$ are constants.

In order to limit the linear and angular velocities sent to the mobile platform, low-pass filters were introduced as follows:

$$\begin{aligned} \tau_v \dot{v}^\star(t) + v^\star(t) &= v(t) \quad (a) \\ \tau_\omega \dot{\omega}^\star(t) + \omega^\star(t) &= \omega(t) \quad (b) \end{aligned} \tag{12}$$

where τ_v, τ_ω are time constants; $v(t)$, $\omega(t)$ are linear and angular velocities calculated from (11); and $v^\star(t)$, $\omega^\star(t)$ are the real commands sent to the mobile platform.

The two charging bars in the back of the mobile platform was connected to the battery poles inside the chassis through a controllable relay, which is normally turned off. The charging bars on the charging station carry a small voltage of $2.5V$ during its standby status. When the robot is backing into the charging location, wheel odometry and ultrasound sensors are implemented to estimate the distance from the charging station. Voltages between the charging bars of the mobile platform is also being monitored to check the docking status. If the $2.5V$ voltage is detected, the recharging operation is successful, and the relay will be turned on, which will trigger the switch of the charging station from standby to charging status. In the mean while, the backing motion of the mobile platform will also be terminated. If the robot's distance to the charger cannot be reduced any further while the $2.5V$ voltage has not been detected, the autonomous recharging operation is failed and the robot will also terminate its backing motion.

V. EXPERIMENTAL RESULTS

Retro-reflective material and black rubbers are known to have different reflection properties. However, their influence on laser intensity has not been quantitatively reported. In Subsection V-A, experiments were conducted to investigate the laser reflection intensity of the reflective tape. In order to demonstrate the effectiveness of the developed laser intensity-based autonomous docking approach, extensive experiments were conducted using the mobile platform shown in Fig. 1(b), and the experimental results are presented in Subsection V-B.

In these experiments, the parameters implemented are summarized in Table 1. The physical dimensions of the mobile platform and the technical specification of the laser range finder shown in Table 1 were determined by the relevant manufactures. As for the reflective tape, the widths of the black-rubber (w_{br}) and retro-reflective (w_{rr}) sections can be selected according to the laser angular resolution (θ) and the potential detection distance L using (7). The farther of the detection distance and the lower of the laser angular resolution, the wider of these sections on the reflective tapes. Similarly, the distance between the two reflective tapes can also be tuned according to the required detection distance and the laser's angular resolution.

TABLE 1. Parameters implemented during the experiments.

Mobile Platform	Tread width (d_m)	Wheel radius (r)	Footprint radius
	$0.37m$	$0.1m$	$0.26m$
Laser Range Finder	Install offset (dL)	Install height (h)	Install tilt (α)
	$0.215m$	$0.175m$	$5°$
	Minimum Range	Maximum Range	Resolution (θ)
	$0.05m$	$25m$	$0.33°$
Reflective Tapes	Rubber width	Reflector width	Tape distance (d)
	$1.95cm$	$0.9cm$	$0.2m$

A. EXPERIMENTS ON LASER INTENSITY OF THE REFLECTIVE TAPE

To avoid introducing potential errors from the robot odometry, the mobile platform is parked in an open area, and a reflective tape was attached to the middle of a 16.5cm-wide plastic box, which was manually moved around in order to adjust the distance and indexes of the laser beams. The plastic box together with the reflective tape was strategically placed at four different locations, as shown in Fig. 5.

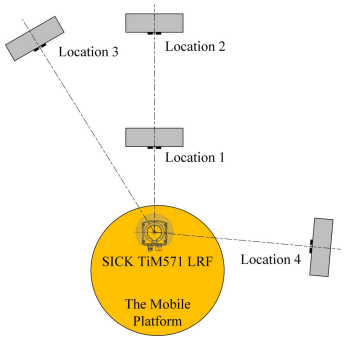

FIGURE 5. Experimental setup for reflective tape detection.

The experimental results are shown in Fig. 6 and Table 2. Figure 6 represents the scan data of the plastic box at the

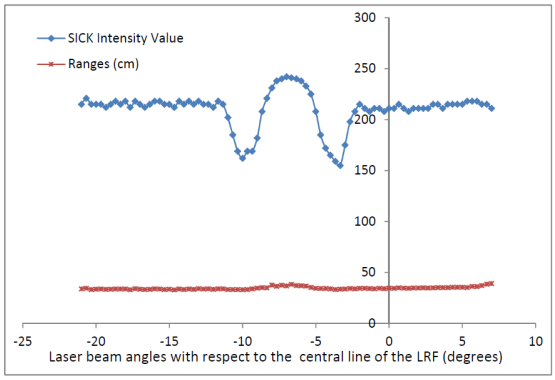

(a) Experimental result for location 1

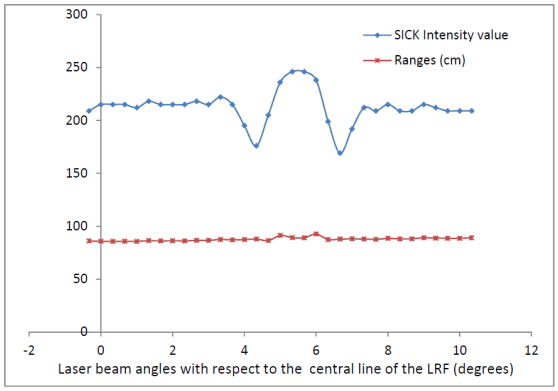

(b) Experimental result for location 2

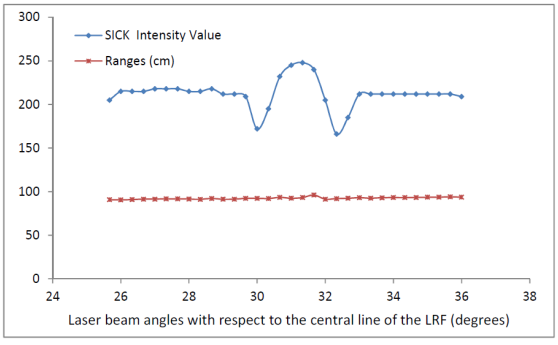

(c) Experimental result for location 3

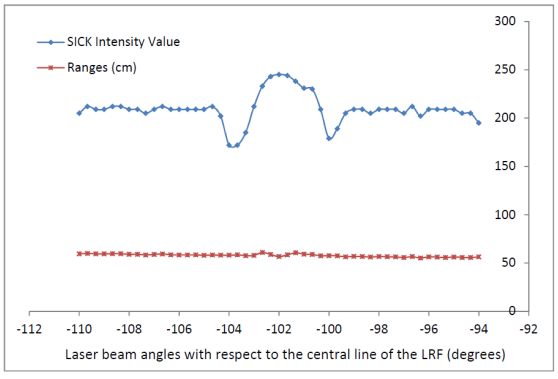

(d) Experimental result for location 4

FIGURE 6. Experiments for reflective tape detection.

four different locations shown in Fig. 5, where the blue lines denote the laser reflection intensity values and the brown lines show the laser range information (i.e., the measured distance from the laser range finder). The markers on these lines represent the laser beams reflected from the plastic box and the reflective tapes. As can be seen from these graphs, the density of reflected laser beams is determined by the distance between the detected object and the laser range finder. For example, the number of reflected laser beams in Fig. 6(a) is much higher than that shown in Figs. 6(b) and (c) because the plastic box was placed much closer to the laser range finder in Location 1 comparing to Location 2 and Location 3, as shown in Fig. 5. From Fig. 6, the diamond retro-reflective area of the reflective tape gave rise to the largest SICK intensity values, which form an obvious peak in the intensity curve. On the other hand, the two black rubber sections of the reflective tape led to the smallest SICK intensity values, which form two valleys beside the aforementioned peak. These features make the reflective tape stand out in the SICK intensity curve, which lays the foundation for the proposed reflector detection technique. In Table 2, the second column presents the range measured by the strongest laser beam, which returned the largest SICK intensity values; the third column shows the angles between the strongest laser beam and the central line of the laser range finder; and the last two columns represent the measured maximum and minimum SICK intensity values.

TABLE 2. Experimental results for reflective tape detection.

Location	Distance	Angles	Maximum Intensity	Minimum Intensity
#1	36.8 cm	$-7°$	242	155
#2	89.2 cm	5.33°	246	169
#3	93.2 cm	31.33°	248	166
#4	56.7 cm	$-102°$	245	172

Remark 5: The experimental results suggest that the difference in materials dominates the detected SICK intensity values, while the influence of distance and laser beam indexes (which determines the angle between a laser beam and the central line of the LRF) is almost negligible in the proposed experimental settings.

B. EXPERIMENTS ON AUTONOMOUS DOCKING

In order to test the developed laser-intensity based autonomous docking approach, two sets of experiments were conducted using the mobile platform shown in Fig. 1(b). The first set of experiments focused on evaluating the performance of the proposed laser-intensity based autonomous docking approach, while the second set of experiments compared the performance of the laser-intensity based autonomous docking approach with a contour-based docking technique.

1) EXPERIMENT #1: TESTING OF THE LASER-INTENSITY BASED AUTONOMOUS DOCKING APPROACH

The first set of experiments were carried out under two different scenarios. In scenario 1, the mobile platform was commanded to charge its battery when it was navigating in one corridor on the left side of the charging station, as shown

in Fig. 7(a). In scenario 2, the mobile platform received the recharging command and started to navigate towards the charging station from the right side, as shown in Fig. 8(a). Herein, left and right sides were defined when one is standing in front of the charging station and facing it.

To test the robustness of the developed autonomous docking approach with varying charging station locations, the charging station was manually moved 20*cm* to the right side along the wall in scenario 2, as shown in Fig. 8. In order to verify the performance of developed approach in dynamic unstructured environments, a person walked between the charger and the mobile platform when it was trying to move towards the intermediate point P in some trials of scenario 2, as shown in Fig. 8(d). To determine the reliability of the developed laser-intensity based autonomous docking approach, experiments were conducted for 200 trials in each scenario. Both autonomous docking and autonomous recharging were monitored. In order to monitor autonomous docking, the charging bars' locations need to be examined. When the charging station switched from standby to charging status, the red light on the charging station will turn on as shown in Figs. 7(f) and 8(f), which provide us with a simple method to monitor autonomous recharging.

The experimental results for the first set of experiments are summarized in Table 3. Snapshots for one sample successful trial in each scenario are shown in Fig. 7 and Fig. 8, respectively. A video is also provided to demonstrate the autonomous docking and recharging procedure in the corresponding trials: https://youtu.be/JuxD8_S3E60.

From the experimental results, the success rates for autonomous docking and autonomous recharging in two different scenarios can be calculated by

$$\begin{aligned} p_{scenario1,docking} &= 99.5\% \\ p_{scenario2,docking} &= 98.5\% \\ p_{scenario1,charging} &= 97.5\% \\ p_{scenario2,charging} &= 96.5\% \end{aligned} \tag{13}$$

Using a two-tailed two proportion z-tests with the level of significance $\alpha = 0.05$ and critical value $Z_{\frac{\alpha}{2}} = 1.96$, the null hypothesis can be defined as H_0 : *the success rates under the two different scenarios are the same*. Similarly, the alternate hypothesis can be defined as $H1$: *the success rates are different for two different scenarios*. The z values for autonomous docking and recharging can be calculated by:

$$\begin{aligned} z_{experiment1,docking} &= 1.005 \\ z_{experiment1,charging} &= 0.586 \end{aligned} \tag{14}$$

Since $-1.96 < 1.005 < +1.96$, $-1.96 < 0.586 < +1.96$, the null hypothesis should be accepted, and it can be concluded that there was no significant difference between the success rates in these two different test scenarios for both autonomous docking and autonomous recharging. In other words, the success rates of the laser-intensity based autonomous docking and recharging approach were not significantly affected by the robot's starting positions, the charger's locations or the uncertainties caused by moving obstacles, confirming the robustness of the proposed laser-intensity based autonomous docking approach.

TABLE 3. Experimental results for the first set of experiments.

Scenario	Scenario 1	Scenario 2
Total number of trials	200	200
Number of successful trials	195	193
Number of trials with failed charging	5	7
Number of trials with failed docking	1	3

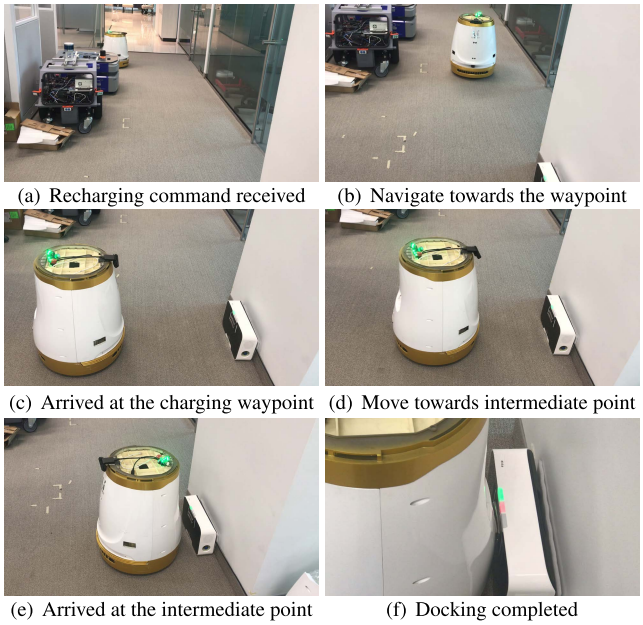

(a) Recharging command received (b) Navigate towards the waypoint (c) Arrived at the charging waypoint (d) Move towards intermediate point (e) Arrived at the intermediate point (f) Docking completed

FIGURE 7. Snapshots for successful docking and recharging in scenario 1.

2) EXPERIMENT #2: LASER-INTENSITY BASED DOCKING APPROACH VERSUS CONTOUR BASED DOCKING TECHNIQUE

In the second set of experiments, the proposed laser-intensity based autonomous docking approach was compared with a contour-based docking technique. The contour-based technique utilized DBSCAN (Density Based Spatial Clustering of Applications with Noise) for clustering of the laser range data, and linear regression algorithm was implemented to predict the coordinates of the charger center. DBSCAN is a density based clustering algorithm, which was developed to cluster data of arbitrary shapes in the presence of noise in spatial and non-spatial high dimensional databases [27]. In the experiments, the DBSCAN parameters were selected as $Eps = 0.03$ and $MinPts = 5$. Details on the DBSCAN algorithm and its parameter selections can be found in [27].

The experiments using both laser-intensity based docking approach and contour-based docking technique were conducted under two different scenarios with similar settings as shown in Fig. 7 and Fig. 8. In scenario 1, the mobile platform started the charging process from the lefts side of

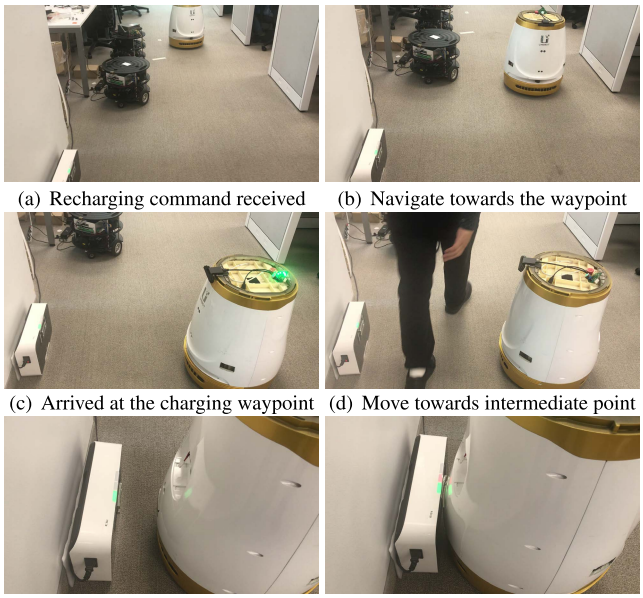

(a) Recharging command received (b) Navigate towards the waypoint
(c) Arrived at the charging waypoint (d) Move towards intermediate point
(e) Arrived at the intermediate point (f) Docking completed

FIGURE 8. Snapshots for successful docking and recharging in scenario 2.

the charging station, and there was no obstacles or confusing objects surrounding the charger. In scenario 2, the mobile platform was ordered to charge its battery from the right side of the charging station, and a person was walking between the charger and the mobile platform to form a dynamic and unstructured environment. Experiments were conducted for 200 trials, and the experimental results are shown in Table 4.

TABLE 4. Experimental results for the second set of experiments.

Docking Methods	laser-intensity approach		contour technique	
	scenario 1	scenario 2	scenario 1	scenario 2
Total number of trials	200	200	200	200
Number of successful trials	195	193	190	165
Number of trials with failed charging	5	7	10	35
Number of trials with failed docking	1	3	5	31

From Table 4, the experimental results for scenario 1 suggested that the success rates for autonomous docking and autonomous recharging using the two different docking methods can be calculated as:

$$\begin{aligned} p_{scenario1,docking,intensity} &= 99.5\% \\ p_{scenario1,docking,contour} &= 97.5\% \\ p_{scenario1,charging,intensity} &= 97.5\% \\ p_{scenario1,charging,contour} &= 95\% \end{aligned} \tag{15}$$

Using two-tailed two proportion z-tests with the level of significance $\alpha = 0.05$ and critical value $Z_{\frac{\alpha}{2}} = 1.96$, it was found that there was no statistically significant difference between the success rates using the two different docking methods for both autonomous docking and autonomous recharging in scenario 1 since $-1.96 < z_{scenario1,docking} = 1.645 < 1.96$ and $-1.96 < z_{scenario1,charging} = 1.316 < 1.96$. The test results confirmed that both the laser-intensity based approach and the contour-based technique demonstrated similar performance for autonomous docking in such structured environment as scenario 1.

From the experimental results for scenario2, the success rates for autonomous docking and recharging using the two different docking methods can be calculated as:

$$\begin{aligned} p_{scenario2,docking,intensity} &= 98.5\% \\ p_{scenario2,docking,contour} &= 84.5\% \\ p_{scenario2,charging,intensity} &= 95\% \\ p_{scenario2,charging,contour} &= 82.5\% \end{aligned} \tag{16}$$

Using upper-tailed two proportion z-tests with the level of significance $\alpha = 0.05$ and critical value $Z_\alpha = 1.645$, the null hypothesis and alternative hypothesis can be defined as H_0 : *both docking methods had the same success rates in scenario2*, and H_1 : *the laser-intensity based approach had higher success rates than the contour-based technique in scenario 2*, respectively. The z values for autonomous docking and autonomous recharging can be calculated by:

$$\begin{aligned} z_{scenario2,docking} &= 5.020 \\ z_{scenario2,charging} &= 4.567 \end{aligned} \tag{17}$$

As $5.020 > 1.645$ and $4.567 > 1.645$, the null hypothesis should be rejected, and it can be concluded that the laser-intensity based approach has higher success rates for autonomous docking and recharging than the contour-based technique in scenario 2, which represents an unstructured environment with dynamic moving obstacles.

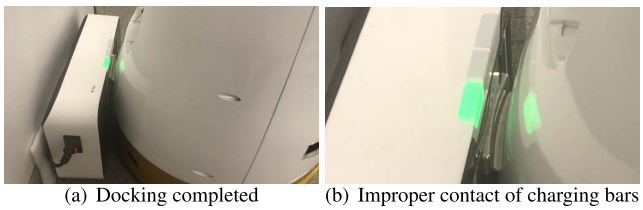

(a) Docking completed (b) Improper contact of charging bars

FIGURE 9. Example trial with successful docking and failed recharging.

3) DISCUSSIONS

For most of the failed autonomous recharging trials in scenario 1, the autonomous docking operations were successful, as shown in Fig. 9(a). However, the charging station tilted, resulting in improper contact of the charging bars, as shown in Fig. 9(b). As a result, the autonomous recharging operation failed because the $2.5V$ voltage mentioned at the end of Section IV was not detected. From the pictures shown in Figs. 7-9, there is a gap between the wall and the upper part of the charging station, which is caused by the carpet covered baseboard at the bottom of the wall. In order to solve the charger tilting issue identified in these failed recharging trials, the charging station needs to be properly mounted.

During the experiments, obvious wheel slippage were noticed, which changed the robot orientation during the backing motion. Furthermore, the turning motion at the intermediate point and the backing motion to the charging station were realized using wheel odometry, which affected the accuracy of autonomous docking, as shown in Fig. 8(f). These motion errors contributed to most of the failed docking trials in scenario 1. In order to reduce or remove the aforementioned motion errors, the charging bars need to be installed in the front side of the mobile platform, so as to allow access to the laser information during the overall docking process.

The control gains for the proportional controller were selected as $k_1 = 0.8$ and $k_2 = 0.5$, which were experienced values. As for the intermediate point P for autonomous docking, it was selected to be $l = 0.4\,m$ away from the center point of the charging station with consideration of the footprint radius of the mobile platform, as well as the open area in front of the charging station. The intermediate point should be selected to allow the mobile platform to make a turn without any collisions. For the mobile platform implemented in this paper, it is not advisable to select a large distance l due to the aforementioned slippage and backing motion errors.

In some of the failed trials for autonomous docking in scenario 2, the person had been blocking the charging station for too long, and the robot failed to detect the reflective tapes while using the proposed laser-intensity based docking approach. As a result, the mobile robot abandoned the autonomous recharging operation due to timeout. These failed trials disclosed one common limitation of all the laser and vision-based approaches, i.e., the charging station has to be within the field of view of the laser range finder or the onboard camera. As for the contour-based docking technique, most of the failed trials in scenario 2 were caused by mistakenly taking the person's legs as part of the charger's cluster, giving rise to incorrect estimation of the charger's location.

For the mobile platform implemented in the experiments, the battery level had been monitored, and autonomous docking and recharging operation would be automatically initialized when the battery voltage drops to below a predefined threshold, e.g., 20% of the maximum value. Besides the autonomous mode, the docking and recharging process can also be triggered manually when an operator sends a charging command through the App or human-robot interaction (HRI) interface. The charging station implemented in these experiments was powered from a wall plug, and the tether had limited the moving range of the charging station. However, the developed autonomous docking and recharging approach can be implemented for tetherless mobile charging stations without any modifications. In practical applications, autonomous charging of mobile robots is a very complicated task, involving calculation of power demand, estimation of the battery's state of charge [28], and placement of charging stations [29]. These important topics are beyond the scope of this paper, which focuses on autonomous docking of mobile robots. During the experiments, the remaining power of the battery was assumed to be sufficient to allow the mobile robot to arrive at the closest charging station when the battery voltages drops to 20% of the maximum value. More details regarding battery state of charge estimation and intelligent charger placement can be found in [28]–[30].

VI. CONCLUSION AND FUTURE RESEARCHES

This paper presents the development of a novel laser reflection intensity based autonomous docking approach, which allows for reliable detection of a charging station in unstructured environments without any requirements on the charger's shape or the contour of objects in its surrounding environments. Sufficient and necessary conditions for reflector detection were derived, which provide a guideline for proper installation of reflectors in practical applications. Physical experiments were conducted to quantitatively investigate the laser reflection intensity of a reflective tape, which lays solid foundation for future research involving laser reflection intensities. Extensive experiments were conducted for autonomous docking of a mobile platform in both structured and unstructured environments. The experimental results confirmed that the performance of the proposed autonomous docking and recharging approach was not affected by the robot's starting position, the charger's location or moving obstacles in unstructured environments. A deep comparative study using z tests validated that the proposed laser intensity based autonomous docking and recharging approach has significant higher success rates than a contour-based technique in unstructured environments. The reflective tapes are affordable and easy to deploy, making the proposed autonomous docking approach easier to accept by industry than the other high-cost solutions.

In my future research, more experiments will be conducted in order to test the developed approaches with different kinds of reflective tapes and laser range finders using various mobile platforms in more complicated scenarios. In particular, the influence of dynamic light, different barrier materials (e.g., glass) and sunlight effects in outdoor environments will be investigated. Furthermore, the developed autonomous docking approach will be extended to warehouse applications for autonomous pallet pickup, which forms another important part of my future research.

ACKNOWLEDGMENT

Some experiments were conducted when the author was working as the team lead of Autonomous Navigation Division at Engineering Service Inc., Markham, ON, Canada. Technical support from John Song is highly appreciated.

REFERENCES

[1] F. Guangrui and W. Geng, "Vision-based autonomous docking and recharging system for mobile robot in warehouse environment," in *Proc. 2nd Int. Conf. Robot. Autom. Eng. (ICRAE)*, Shanghai, China, Dec. 2017, pp. 79–83.

[2] J. Miseikis, P. Caroni, P. Duchamp, A. Gasser, R. Marko, N. Miseikiene, F. Zwilling, C. de Castelbajac, L. Eicher, M. Fruh, and H. Fruh, "Lio—A personal robot assistant for human–robot interaction and care applications," *IEEE Robot. Autom. Lett.*, vol. 5, no. 4, pp. 5339–5346, Oct. 2020.

[3] R. C. Luo, C. T. Liao, and K. C. Lin, "Vision-based docking for automatic security robot power recharging," in *Proc. IEEE Workshop Adv. Robot. Social Impacts*, Nagoya, Japan, Jun. 2005, pp. 214–219.
[4] G. Liu, Y. Liu, H. Zhang, X. Gao, J. Yuan, and W. Zheng, "The Kapvik robotic mast: An innovative onboard robotic arm for planetary exploration rovers," *IEEE Robot. Autom. Mag.*, vol. 22, no. 1, pp. 34–44, Mar. 2015.
[5] Y. Liu and G. Nejat, "Robotic urban search and rescue: A survey from the control perspective," *J. Intell. Robot. Syst.*, vol. 72, no. 2, pp. 147–165, Nov. 2013.
[6] B. Doroodgar, Y. Liu, and G. Nejat, "A learning-based semi-autonomous controller for robotic exploration of unknown disaster scenes while searching for victims," *IEEE Trans. Cybern.*, vol. 44, no. 12, pp. 2719–2732, Dec. 2014.
[7] Y. Liu and G. Nejat, "Multirobot cooperative learning for semiautonomous control in urban search and rescue applications," *J. Field Robot.*, vol. 33, no. 4, pp. 512–536, Jun. 2016.
[8] M. C. Silverman, D. Nies, B. Jung, and G. S. Sukhatme, "Staying alive: A docking station for autonomous robot recharging," in *Proc. IEEE Int. Conf. Robot. Autom.*, Washington, DC, USA, May 2002, pp. 1050–1055.
[9] M. Doumbia, X. Cheng, and V. Havyarimana, "An auto-recharging system design and implementation based on infrared signal for autonomous robots," in *Proc. 5th Int. Conf. Control, Autom. Robot. (ICCAR)*, Beijing, China, Apr. 2019, pp. 894–900.
[10] U. Kartoun, H. Stern, Y. Edan, C. Feied, J. Handler, M. Smith, and M. Gillam, "Vision-based autonomous robot self-docking and recharging," in *Proc. World Autom. Congr.*, Bduapest, Hungary, Jul. 2006, pp. 1–8.
[11] R. C. Luo, C. T. Liao, and S. C. Lin, "Multi-sensor fusion for reduced uncertainty in autonomous mobile robot docking and recharging," in *Proc. IEEE/RSJ Int. Conf. Intell. Robots Syst.*, St. Louis, MO, USA, Oct. 2009, pp. 2203–2208.
[12] Mobile Industrial Robots A/S. *MiRCharge 24V*. Accessed: Jul. 3, 2022. [Online]. Available: https://www.mobile-industrial-robots.com/solutions/mir-applications/mir-charge-24v
[13] Fetch Robotics. *Tutorial: Auto Docking*. Accessed: May 24, 2022. [Online]. Available: https://docs.fetchrobotics.com/docking.html
[14] W. G. Walter, *The Living Brain*. New York, NY, USA: W. W. Norton, 1953.
[15] S. Roh, J. H. Park, Y. H. Lee, Y. K. Song, K. W. Yang, M. Choi, H.-S. Kim, H. Lee, and H. R. Choi, "Flexible docking mechanism with error-compensation capability for auto recharging system of mobile robot," *Intl. J. Control, Autom. Syst.*, vol. 6, no. 5, pp. 731–739, Oct. 2008.
[16] R. Quilez, A. Zeeman, N. Mitton, and J. Vandaele, "Docking autonomous robots in passive docks with infrared sensors and QR codes," in *Proc. Int. Conf. Testbeds Res. Infrastruct. Develop. Netw. Communities*, Vancouver, BC, Canada, Jun. 2015, Paper hal-01147332.
[17] M. V. S. Rao and M. Shivakumar, "Sensor guided docking of autonomous mobile robots for battery recharging," *Intl. J. Recent Technol. Eng.*, vol. 8, no. 4, pp. 3515–3812, 2019.
[18] A. M. Burgueño-Romero, J. R. Ruiz-Sarmiento, and J. Gonzalez-Jimenez, "Autonomous docking of mobile robots by reinforcement learning tackling the sparse reward problem," in *Advances in Computational Intelligence*, vol. 12862, I. Rojas, G. Joya, and A. Català, Eds. Cham, Switzerland: Springer, 2021, pp. 392–403.
[19] K.-T. Song, C.-W. Chiu, L.-R. Kang, Y.-X. Sun, and C.-H. Meng, "Autonomous docking in a human–robot collaborative environment of automated guided vehicles," in *Proc. Int. Autom. Control Conf. (CACS)*, Nov. 2020, pp. 1–6.
[20] S. Khan, D. Wollherr, and M. Buss, "Modeling laser intensities for simultaneous localization and mapping," *IEEE Robot. Autom. Lett.*, vol. 1, no. 2, pp. 692–699, Jul. 2016.
[21] G. Wu, J. Wang, H. Wang, L. Xie, and P. Li, "An improved scan matching method based on laser reflection intensity," in *Proc. 10th Int. Conf. Intell. Control Inf. Process. (ICICIP)*, Marrakesh, Morocco, Dec. 2019, pp. 51–58.
[22] A. Carballo, A. Ohya, and S. Yuta, "People detection using range and intensity data from multi-layered laser range finders," in *Proc. IEEE/RSJ Int. Conf. Intell. Robots Syst.*, Taipei, Taiwan, Oct. 2010, pp. 5849–5854.
[23] H. Wang, C. Wang, and L. Xie, "Intensity-SLAM: Intensity assisted localization and mapping for large scale environment," *IEEE Robot. Autom. Lett.*, vol. 6, no. 2, pp. 1715–1721, Apr. 2021.
[24] SICK. *2D LiDAR Sensors TiM5xx*. Accessed: May 24, 2022. [Online]. Available: https://www.sick.com/ca/en/detection-and-ranging-solutions/2dlidar-sensors/tim5xx/tim571-2050101/p/p412444
[25] G. Grisetti, C. Stachniss, and W. Burgard, "Improved techniques for grid mapping with rao-blackwellized particle filters," *IEEE Trans. Robot.*, vol. 23, no. 1, pp. 34–46, Feb. 2007.
[26] Open Robotics. *ROS Navigation Stack*. [Online]. Available: http://wiki.ros.org/navigation
[27] M. Ester, H.-P. Kriegel, J. Sander, and X. Xu, "A density-based algorithm for discovering clusters in large spatial databases with noise," in *Proc. 2nd Int. Conf. Knowl. Discovery Data Mining*, Portland, OR, USA, Aug. 1996, pp. 226–231.
[28] M. Partovibakhsh and G. Liu, "An adaptive unscented Kalman filtering approach for online estimation of model parameters and state-of-charge of lithium-ion batteries for autonomous mobile robots," *IEEE Trans. Control Syst. Technol.*, vol. 23, no. 1, pp. 357–363, Jan. 2015.
[29] T. Kundu and I. Saha, "Charging station placement for indoor robotic applications," in *Proc. IEEE Int. Conf. Robot. Autom. (ICRA)*, May 2018, pp. 3029–3036.
[30] T. Kundu and I. Saha, "SMT-based optimal deployment of mobile rechargers," in *Proc. IEEE Int. Conf. Robot. Autom. (ICRA)*, May 2021, pp. 8165–8171.

YUGANG LIU (Member, IEEE) received the B.E. degree from the University of Science and Technology, Beijing, China, in 1999, the M.A.Sc. degree from the Beijing University of Posts and Telecommunications, Beijing, in 2002, and the Ph.D. degree from the University of Toronto, ON, Canada, in 2019.

From 2002 to 2006, he was a Research Assistant with the Faculty of Science and Technology, University of Macau, Macao, China. From 2006 to 2012, he was a Research Associate with the Department of Aerospace Engineering, Ryerson University, Toronto, ON, Ontario, Canada. From 2017 to 2020, he was a Team Lead with the Autonomous Navigation Division, Engineering Service Inc. (ESI), Toronto. Since May 2020, he has been an Assistant Professor with the Department of Electrical and Computer Engineering, Royal Military College of Canada, Kingston, ON, Canada. He has authored or coauthored more than 40 articles in international journals and conference proceedings. His research interests include autonomous navigation, autonomous exploration, learning-based robotics control, mobile manipulation, and robotic search and rescue. He was a recipient of the IFAC *Mechatronics* Journal Best Paper Award, in 2014.